

2022

## Fabrication and Characterization of Methylprednisolone-Loaded Polylactic Acid/Hyaluronic Acid Nanofibrous Scaffold for Soft Tissue Engineering

Mehdi Keikha  
*Tehran University of Medical Sciences*

Elahe Entekhabi  
*Amirkabir University of Technology*

Mahvash Shokrollahi  
*Amirkabir University of Technology*

Masoumeh Haghbin Nazarpak  
*Amirkabir University of Technology*

Follow this and additional works at: [https://jdc.jefferson.edu/rothman\\_institute](https://jdc.jefferson.edu/rothman_institute)

Zahra Hassannejad  
 *Tehran University of Medical Sciences*  
Part of the [Medical Biotechnology Commons](#)

**[Let us know how access to this document benefits you](#)**

*See next page for additional authors*

---

### Recommended Citation

Keikha, Mehdi; Entekhabi, Elahe; Shokrollahi, Mahvash; Nazarpak, Masoumeh Haghbin; Hassannejad, Zahra; Akbari, Somaye; Vaccaro, Alex R.; and Rahimi-Movaghar, Vafa, "Fabrication and Characterization of Methylprednisolone-Loaded Polylactic Acid/Hyaluronic Acid Nanofibrous Scaffold for Soft Tissue Engineering" (2022). *Rothman Institute Faculty Papers*. Paper 187.  
[https://jdc.jefferson.edu/rothman\\_institute/187](https://jdc.jefferson.edu/rothman_institute/187)

This Article is brought to you for free and open access by the Jefferson Digital Commons. The Jefferson Digital Commons is a service of Thomas Jefferson University's [Center for Teaching and Learning \(CTL\)](#). The Commons is a showcase for Jefferson books and journals, peer-reviewed scholarly publications, unique historical collections from the University archives, and teaching tools. The Jefferson Digital Commons allows researchers and interested readers anywhere in the world to learn about and keep up to date with Jefferson scholarship. This article has been accepted for inclusion in Rothman Institute Faculty Papers by an authorized administrator of the Jefferson Digital Commons. For more information, please contact: [JeffersonDigitalCommons@jefferson.edu](mailto:JeffersonDigitalCommons@jefferson.edu).

---

**Authors**

Mehdi Keikha, Elahe Entekhabi, Mahvash Shokrollahi, Masoumeh Haghbin Nazarpak, Zahra Hassannejad, Somaye Akbari, Alex R. Vaccaro, and Vafa Rahimi-Movaghar

# Fabrication and characterization of methylprednisolone-loaded polylactic acid/hyaluronic acid nanofibrous scaffold for soft tissue engineering

Volume 52: 1–24

© The Author(s) 2022





Article reuse guidelines:

[sagepub.com/journals-permissions](https://sagepub.com/journals-permissions)

DOI: 10.1177/15280837221116593

[journals.sagepub.com/home/jit](https://journals.sagepub.com/home/jit)

Mehdi Keikha<sup>1,2</sup>, Elahe Entekhabi<sup>3</sup>, Mahvash Shokrollahi<sup>4</sup>, Masoumeh Haghbin Nazarpak<sup>4</sup> , Zahra Hassannejad<sup>5</sup>, Somaye Akbari<sup>6</sup> , Alex R Vaccaro<sup>7</sup> and Vafa Rahimi-Movaghar<sup>1</sup>

## Abstract

Previous in vitro and in vivo studies have indicated that tissue engineering scaffolds, including Schwann cells, may improve axonal regeneration, particularly in combination with Methylprednisolone as an influential neuroprotective factor. The primary aim of this study was to design composite electrospun scaffolds based on polylactic acid (PLA)/hyaluronic acid (HA) containing various percentages (0.05–2% (w/v)) of Methylprednisolone (MP) with suitable mechanical and chemical properties for soft tissue especially to promote nerve growth. For the first time, MP was implicated in a PLA/HA nanofibrous and its effect on fiber's properties was scrutinized as a candidate for nerve tissue

<sup>1</sup>Sina Trauma and Surgery Research Center, Tehran University of Medical Sciences, Tehran, Iran

<sup>2</sup>Chemical Engineering Department, Amirkabir University of Technology, Tehran, Iran

<sup>3</sup>Biomedical Engineering Department, Amirkabir University of Technology, Tehran, Iran

<sup>4</sup>New Technologies Research Center (NTRC), Amirkabir University of Technology, Tehran, Iran

<sup>5</sup>Pediatric Gene, Cell & Tissue Research Center, Tehran University of Medical Sciences, Tehran, Iran

<sup>6</sup>Textile Engineering Department, Amirkabir University of Technology, Tehran, Iran

<sup>7</sup>Department of Orthopedics and Neurosurgery, Rothman Institute, Thomas Jefferson University, Philadelphia, PA, USA

## Corresponding authors:

Masoumeh Haghbin Nazarpak, New Technologies Research Center, Amirkabir University of Technology, Hafez Street, Tehran 15875, Iran.

Email: [haghbin@aut.ac.ir](mailto:haghbin@aut.ac.ir)

Vafa Rahimi-Movaghar, Sina Trauma and Surgery Research Center, Tehran University of Medical Sciences, Tehran 1416753955, Iran.

Email: [v\\_rahimi@sina.tums.ac.ir](mailto:v_rahimi@sina.tums.ac.ir)

engineering. In addition, morphology, chemical bonding, wettability, and degradation of the scaffolds were examined to evaluate their performance. The results showed the PLA/HA scaffolds had suitable morphological, physicochemical, and mechanical properties for nerve regeneration. Also, various percentages of MP were evaluated through physicochemical assay, drug release profile, and biological assays to find an optimum level of drug. These scaffolds may improve the growth and viability of Schwann cells. Results showed that composite scaffolds containing 0.5 w/v MP had lower cytotoxicity and higher biocompatibility.

### Keywords

nanofibrous scaffold, Schwann cell, methylprednisolone, nerve regeneration, polylactic acid, hyaluronic acid

## Introduction

Many people around the world suffer from nerve tissue damage that it may not be possible to prevent. Unfortunately, one of the most significant drawbacks of nerve damage is that these cells have a low healing capability, and injured tissue cannot be repaired on its own, which is maybe due to the secretion of many inflammatory agents at the site of injury.<sup>1</sup>

For decades, literature has supported the extracellular matrix (ECM) role in the intracellular function and cell-to-cell communication.<sup>2</sup> Tissue engineering scaffolds can mimic the role of ECM by providing a similar microenvironment through their unique physicochemical and biological properties.<sup>3</sup>

It is well described in previous studies by a great number of researchers in the last decades, which the role of the structure of ECM in cell proliferation<sup>1,4</sup> and how the synthetic and natural polymer will affect this situation<sup>5,6</sup>

As Lotfi et al. said, every cell has a unique environment with specific physical architecture and chemical features. In this aspect, it is important to provide an environment both on nano and microscale for Schwann cells similar to the natural peripheral nerve system. In addition, nano-fibrous architecture showed a promising improvement in a large variety of nervous post-implantation effects, owing to mimicry of nanostructure in ECM.<sup>6,7</sup>

In the past, many scaffolds have been used in soft tissue engineering like nerve tissue engineering, and electrospun nanofibers are regarded as one of the most attractive methods of repairing damaged tissue due to their unique properties.<sup>1</sup>

Electrospun nanofibrous scaffolds providing a high-specific surface area and high porosity to mimic the ECM and support nerve cell behaviors<sup>3,8,9,6</sup> are good choices for neural tissue engineering. The advantages of electrospinning in scaffold fabrication include (1) the ability to control fiber diameter, porosity, and pore size, and (2) the ability to use different types of natural and synthetic polymers.<sup>10,11,12</sup>

Adjustable features of the electrospinning method together with simplicity and cost-effectiveness made this method a favorable way of conduits production insight of

industrial.<sup>13</sup> Large-scale production is another interesting characteristic of electrospinning to be mentioned.

Polymeric materials have been widely used as constituents for *in vitro* and *in vivo* nerve tissue regeneration.<sup>9,14,15</sup> Poly (lactic acid) or poly (lactide) (PLA) is biodegradable and one of the most widely used synthetic biopolymers in biomedical applications.<sup>10,16</sup> PLA is produced from the polymerization of the cyclic dimer lactide versatility.<sup>10</sup> The cytocompatibility and biodegradability of PLA make it an appropriate candidate for tissue engineering scaffolds and implantable devices.<sup>10,17,18</sup> Moreover, the degradation rate of PLA is slow, and its weight loss in the simulated body solution over 28 days is less than 0.2%.<sup>19</sup> Biodegradable PLA has suitable physicochemical properties and relatively good biocompatibility for biomedical engineering. Nevertheless, PLA has some drawbacks, such as poor cell adhesion, biological inertness, slow degradation rate, and acidic degradation by-products. Among all these properties, cell adhesion is a critical factor for a promising scaffold that must be satisfied. The hydrophobic nature of PLA along with the lack of functional groups make it difficult for cells to adhere to the scaffold.<sup>20</sup> Characteristics of PLA can be strengthened by combining with a polymer with high biological properties.<sup>21</sup>

On the other hand, hyaluronic acid or hyaluronan (HA) is a natural polysaccharide and one of the main ECM components in the nerve tissue that includes  $\beta$ -1, 3-N-acetyl-D-glucosamine and  $\beta$ -1,4-D-glucuronic acid units.<sup>22,23,24</sup> HA is a highly hydrophilic polymer that interacts with cell surface receptors like the RHMM15 and CD44.<sup>25,26</sup> In addition, HA plays a significant role in elevating the production of transforming growth factor  $\beta$ 1.<sup>27</sup> The molecular weight of HA generally exceeds 10<sup>6</sup> Da.<sup>28</sup> Obviously, the structural, physical, physicochemical, biological, and degradable properties of HA depend entirely on its molecular weight.<sup>29</sup>

Moreover, HA improves cell-matrix interactions, specifically increasing neural cell proliferation, according to cell studies.<sup>1</sup> This finding is due to the natural properties of HA, which could mimic the ECM conditions for neural cells. Also, the evidence shows that in combination with polyelectrolytes or proteins HA supports Schwann cells' growth and proliferation.<sup>30,31</sup> In addition, the efficient role of HA in wound healing, and reduction of glial scar formation have been reported which is attractive in repairing damaged nerves.<sup>11,23</sup> Schwann cells are the most structural cell in the peripheral nerve system. Biocompatible scaffolds had been indicated as an alternative option instead of the conventional clinical method such as autografts, allografts, and xenografts for soft tissue regeneration. Each of these strategies has obstacles in the healing process. For instance, the chance of immune response and low reproducibility limited the implication of allografts and xenografts.<sup>43</sup>

For an ideal tissue-engineered scaffold mimicking the extracellular matrix (ECM) is a critical factor. Hence, providing an adequate network for Schwann cells in which they could adhere, migrate and proliferate is an important factor for a promising scaffold.

In this study, the mechanical and physicochemical properties of PLA/HA electrospun nanofibrous have been evaluated to be a novel candidate for nerve regeneration scaffold. Also, electrospun PLA fibers have been used in combination with PCL polymer in several

studies to improve nerve tissue, and its various features have been explored.<sup>32,33</sup> These are two of the most widely used synthetic polymers used in nerve tissue engineering history.

Although nanofibrous PLA/HA-based scaffold produced by electrospinning was prepared and scrutinized for vascular tissue engineering in a previous study by Niu et al.,<sup>34</sup> desired properties for nerve tissue are quite different due to their different morphological characteristics. Niu et al.<sup>34</sup> focused on cardiac tissue engineering and angiogenesis, and they have not employed any drugs or growth factors, and its cytotoxicity was not adequately evaluated. However, the results showed that the scaffold could simulate the ECM environment well for the desired cell line.

Methylprednisolone is a synthetic corticosteroid drug that enhances anti-inflammatory activity and reduces mineralocorticoid activity analogous to cortisol.<sup>35,36</sup> MP is an influential neuroprotective factor limiting lipid peroxidation and lessens the post-traumatic degenerative process that ensues following neural injury.<sup>37–39</sup> Also, MP improves blood flow and reduces lactate levels. It may inhibit free radical production after trauma and help recover neurological function.<sup>40</sup> Researchers have also shown that MP has an influential role in axonal regeneration and delays scar formation in peripheral nerves in rat models.<sup>41</sup>

In addition, MP exerted neuroprotective effects against oxidative damage by suppressing autophagy and apoptosis.<sup>42</sup> Extensive studies of the pharmacological effect of MP on nerve tissue regeneration make it an effective option for our purpose. The ultimate goal of this work is to produce polymeric nanofiber with appropriate properties as a promising candidate for soft tissue engineering, especially for nerve regeneration. Hence, MP is used as a neuroprotective factor that inhibits inflammatory and autophagy in Schwann cells.

In this study, the properties of PLA electrospun scaffolds improved by blending with HA; then, MP was loaded in an attempt to enhance Schwann cell behaviors, aiding in nerve tissue regeneration. The distinguishing feature of our research is the use of methylprednisolone, which has good anti-inflammatory properties and improves the healing process in damaged nerve cells. After examining the mechanical and physicochemical properties of the scaffold, the cell viability and adhesion of nerve cells responding to the scaffolds were examined to determine the optimal drug concentration.

## Materials and methods

### Materials

PLA ( $M_w = 6.8 \times 10^5$ ) and HA ( $M_w = 1.2 \times 10^6$ ) were purchased from Bohring, Inc German and Sigma–Aldrich (St Louis, MO), respectively. Chloroform (CF) and dimethylformamide (DMF) were supplied from Merck (Darmstadt, Germany) and Methylprednisolone was provided from Ronak Pharmaceutical company (Tehran, Iran).

### Preparation of scaffolds

Initial solutions were prepared by dissolving 10% (w/v) PLA and HA with weight ratios of 100:0 and 95:5, in CF: DMF with a volume ratio of 75:25, and stirred for 4 hours at room

temperature. Then, in accordance with Table 1, various percentages of MP, (0.05–2% (w/v)) were added into an HA-containing polymer solution, and stirred for 20 min at room temperature. Finally, the solution was transferred in a 5 ml syringe for electrospinning with a 23-gauge needle diameter. The distance between the collector and the syringe needle tip was 14 cm and the drum screen speed rotating was 1250 r/min. Also, for easy collection and maintenance of fibers, aluminum foil was stretched on the collector surface.

The solution flow rate and applied voltages were 0.5 ml/h and 18 kV, respectively.

### *Fourier-transform infrared spectroscopy (FTIR) analysis*

The conformation and chemical compositions of samples were studied using FTIR spectroscopy over a range of 4000–400  $\text{cm}^{-1}$ . FTIR spectra of specimens were obtained with a Nicolet 17DSX FT-IR spectrometer (Thermo Scientific, Waltham, MA). After drawing FTIR charts and analyzing them, the peaks related to the bonds in each compound (which are mostly strong peaks) were identified at specific wavelengths based on the references.

### *Microstructure and morphology analysis*

To study scaffolds microstructure, the  $1 \times 1 \text{ cm}^2$  cut of the electrospun fibers was coated with a thin layer of gold by sputter coater, and then specimens were analyzed by scanning electron microscope (SEM) (AIS2100; Seron Technology, Uiwang-si, Gyeonggi-do, South Korea) using the voltage of 20 kV. The average fiber diameter was measured using image analysis software (Image J, National Institutes of Health, USA).

### *Water absorption analysis*

In water absorption experiments, the prepared electrospun nanofibrous scaffolds ( $1.5 \times 1.5 \text{ cm}$ ) were immersed in phosphate-buffered saline (PBS) and incubated at  $37^\circ\text{C}$  for 24 h and 48 h. Afterward, the samples were removed from the PBS container, and the PBS on the surface of the samples was detached with tissue paper and then reweighed.<sup>29</sup>

**Table 1.** Sample code based on the amount of drug-loaded.

Sample code	MP (%wt.)
P0.05	0.05
P0.1	0.1
P0.2	0.2
P0.5	0.5
P1	1
P2	2

The water: absorption value (S) of the samples was calculated using the following equation:

$$S = \left[ \frac{w_w - w_d}{w_d} \right] \times 100 \quad (1)$$

Where,  $W_w$  is the wet weight of samples and  $W_d$  is the dried weight of samples, respectively.

### *Mechanical properties*

Mechanical properties of the scaffolds, including elongation and tensile strength, were determined using a tabletop uniaxial testing machine (Instron 5566, USA) at room temperature according to American standards for testing methods (ASTM-D882). According to the reported method.<sup>44</sup> Briefly, a square paper frame with  $5 \times 5$  cm outer and  $3 \times 3$  cm inner dimensions was prepared, then the electrospun fiber was cut to a  $4 \times 1$  cm strip and adhered to the center of the frame. The prepared samples were mounted on the wedge grips and the force was applied. A stress-strain curve was drawn to calculate the ultimate tensile strength and elongation of samples. Three samples were tested for statistical evaluations.

### *Degradation analysis*

The physical integrity of the scaffolds was obtained in PBS at pH 7.4 at  $37^\circ\text{C}$  at different time intervals (3, 7, 14, 21, and 28 days). After removing the solution, samples were rinsed with deionized water and dried. Then, the microstructure of the samples was observed by SEM to evaluate the morphological changes within 28 days.

The degradation rate of the nanofibrous samples was determined by measuring the weight loss of the samples for 2 weeks. After measuring the weight of dry samples ( $M_i$ ), they were immersed in a 20 ml PBS (pH 7.4 at  $37^\circ\text{C}$ ) and underwent an incubation process at different time intervals (7 and 14 days) according to American standards for testing methods (ASTM- F1635-11). After that, the samples were retrieved, washed with distilled water, fully dried in vacuum, and weighed ( $M_d$ ) to measure the weight loss. At each time point of incubation, the PBS solution was exchanged for a fresh one. The weight loss percentage of mats was measured:<sup>45</sup>

$$\Delta W = \frac{M_i - M_d}{M_i} \times 100 \quad (2)$$

### *Drug release studies*

The MP release from electrospun nanofibrous scaffolds was evaluated by cutting 0.01 mg of MP-loaded fiber scaffolds to  $1 \times 1 \text{ cm}^2$  and placing them within an active dialysis bag



containing 5 ml PBS, then keeping them at 37°C in a beaker containing 30 ml PBS (pH 7.4) and stirring them constantly.

Drug release was assessed at different time intervals over 240 h. At specified time intervals, 3 ml of the PBS solution was removed and replaced with a fresh one. The removed solution was used to measure the released drug by UV spectrophotometer (Cary 100bio, Varian) at a wavelength of 260 nm.

At each time point, the late corresponding concentration of release MP with regard to the standard curve of MP was recorded. The following equation assessed the percentage of the cumulative release of MP ( $E_r$ ):

$$\%E_r = \frac{V_o \times C_n + V_r \times \sum_1^{n-1} C_i}{M_t} \times 100 \quad (3)$$

Where,  $V_o$  and  $V_r$  are the volumes of the release media and the replaced media.  $M_t$  is the MP content encapsulated in the nanofiber scaffold or mat, and  $C_n$  is the MP concentration in the sample<sup>46,47</sup>

### Schwann cell culture

The metabolic activity of Schwann cells (SCs) on the scaffolds was quantified using the MTT assay. SCs were extracted from the 2 to 3 days-old Wistar rat's sciatic nerves and purified according to M. Rajabi et al.<sup>48</sup> and M. Nategh et al.<sup>49</sup> protocol. Briefly, sciatic nerves were extracted, the epineurium was removed, and after that, nerves were split into several explants and placed in PDL-coated plates. The culture medium of DMEM/F12 supplemented with FBS (10%), penicillin/streptomycin, and 20 mg/mL of BPE was added to the plates, and then the plates were incubated at 37°C in a humidified 5% CO<sub>2</sub> chamber. The explants were sub-cultured 2 to 3 times during 2 weeks. The explants were then digested with 0.125% collagenase and 0.125% trypsin-EDTA and seeded on tissue culture plates for further expansion.

Scaffolds were cut into circles with a diameter of 5 mm and then sterilized ( $n = 6$  for each group). The samples were immersed in aqueous ethanol (70%) at room temperature for 30 min at room temperature for sterilization. Afterward, each side of the sample was exposed to ultraviolet light for 30 min and then washed three times with sterilized PBS. After sterilization, the cells were seeded on scaffolds ( $n = 11 \times 10^4$  cells per sample). Subsequently, the cell culture medium was removed, and 100  $\mu$ l of MTT solution (0.5 mg/ml in PBS) was added to each well. The plates were incubated for 3 and 7 days at 37°C. MTT solution was carefully replaced by 200  $\mu$ l DMSO, and the plates were gently agitated until the formed dark blue formazan crystals were dissolved, and the absorbance of the solution was measured at 570 nm. Also, the 10 mm diameter glass coverslips coated with collagen molecules were used as the control.

Morphology of the cells on the scaffolds was observed by SEM image. For this purpose, the samples containing 0.2 and 0.5% MP were selected as the optimum samples. After 48 h of SCs culture on the scaffolds; the samples were washed twice with PBS and fixed in 2% glutaraldehyde for 40 min at four°C. The samples were rinsed in PBS after

fixation and dehydrated in increasing concentrations of ethanol (70–100%). After that, the samples were dried and coated with a thin layer of gold before cell morphology observation by SEM.

### Statistical analysis

The statistical comparison between different groups was performed using one-way analysis of variance (ANOVA), and the differences were considered significant when  $p$  values  $<0.05$ . All data were presented as mean  $\pm$  standard deviation (SD).

## Results and discussion

In this study, fibrous PLA/HA composite scaffolds loaded with MP were fabricated for the first time via electrospinning. HA was added to the PLA to evaluate the extent of water absorption, mechanical properties, degradation rate, and cell behavior. Furthermore, the effect of MP-loaded PLA/HA nanofibrous scaffolds on SCs growth was studied.

Following a previous study by our group<sup>12</sup> on polycaprolactone/hyaluronic acid polymer nanofibers and the other reports in the literature, it can be concluded that the optimal concentration of hyaluronic acid is 10%. This value is obtained according to the results of cytotoxicity and mechanical assays.

### FTIR Analysis

Chemical analysis was done using FTIR spectroscopy. Figure 1 indicates the spectra of various materials (PLA, HA, MP, and PLA/HA-MP), with the strong peaks highlighted. Infrared spectra of blended PLA/HA-MP samples showed intense absorption peaks at  $1754\text{ cm}^{-1}$  and  $1182\text{ cm}^{-1}$ , which related to the stretching vibrations of the C-O bond and C = O bonds. Moreover, the  $\text{CH}_3$  asymmetric bending peak and the O-H bending peak of PLA are observed at  $1454\text{ cm}^{-1}$  and  $1047\text{ cm}^{-1}$ , respectively.<sup>50,51</sup> The peak at  $1611\text{ cm}^{-1}$  belongs to the presence of the amide group, and the absorption peak at  $2900\text{ cm}^{-1}$  is related to the C-H stretching bond. In addition, the broad absorption peak at  $\sim 3400\text{ cm}^{-1}$  corresponds to O-H stretching bond and confirms the presence of an amino group.<sup>51,52</sup> O-H groups' attendance in HA molecules increases water absorption and improves the interaction between cells and scaffolds.<sup>24,53</sup>

Absorption bands at  $1652.88$  and  $1593.09\text{ cm}^{-1}$  corresponded to the FTIR spectrum of MP.<sup>54</sup> The FTIR spectra of MP showed sharp peaks at  $1715.7\text{ cm}^{-1}$  indicating C=O (ketone), at  $1650\text{--}1550\text{ cm}^{-1}$  indicating C=C (alkenes), and a broad absorption peak between  $3400$  and  $3100\text{ cm}^{-1}$  indicated O-H (alcohol).<sup>55</sup> C=C (ketone) absorption peak near  $1715\text{ cm}^{-1}$  is related to drug structure in PLA/HA-MP composite. FTIR result of the PLA/HA-MP sample shows that PLA and HA are the main components of the final sample and the MP was loaded on nanofiber successfully.

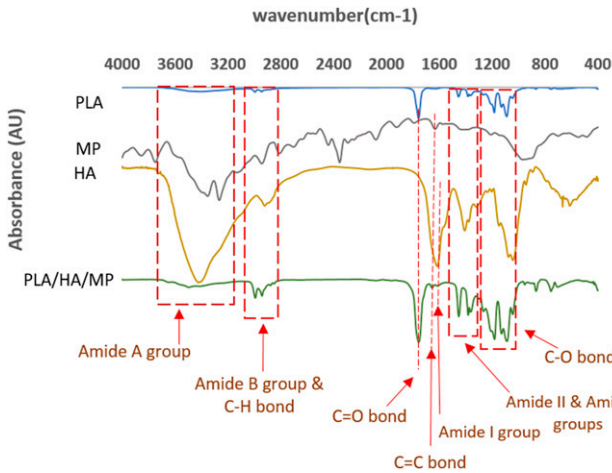


**Figure 1.** Fourier-transform infrared (FTIR) spectra of PLA, MP, HA, PLA/HA/MP

### Morphology and microstructure

Figure 2 shows SEM images of pure PLA and PLA/HA electrospun composite scaffolds along with the average fiber diameter of scaffolds. The micrographs demonstrate that the average fiber diameter of the PLA scaffold is very low (less than 90 nm), and in the PLA/HA composite sample, the average fiber diameter is less than ~30 nm, which was significantly reduced by the presence of HA in the structure compared to the pure PLA sample ( $p < 0.05$ ).

For nerve tissue engineering and cell-matrix interaction, fiber diameter is critical. Because brain cells are long and thin, they require scaffolds with a smaller diameter and greater specific area to mimic their ECM.<sup>1</sup> Many factors may control the nanofiber diameters, including properties of the polymer and solvent system used, as well as electrospinning variables like voltage and flow rate. Since the solvent used for all the solutions in this study was a constant ratio of CF: DMF, the presence of HA in the composite sample is the main reason for the decrease in fiber diameter due to the high number of hydrophilic groups. The polarity of the solution plays an important role in reducing the diameter of the fibers.<sup>12</sup> The presence of HA may account for the increased polarity of the solution and decreasing final fiber diameter. During the electrospinning process, the electric field has more significant effects on polar solution due to increased velocity of the solution stretching which reduces the diameter of fibers.<sup>56</sup> Similar observation on the decrease of fiber diameter upon mixing of HA was also reported by other researchers.<sup>12,57</sup> Higher scaffold contact sites with the environment result from smaller fiber diameter. Thus, by decreasing the fibers' diameter, the specific surface area of the scaffolds increases and leads to higher fiber permeability and a faster degradation rate.<sup>12</sup> Adding HA would also increase the surface area. High surface area promotes protein adsorption and provides more adhesion sites for cell receptors in a biological aspect.<sup>58</sup>

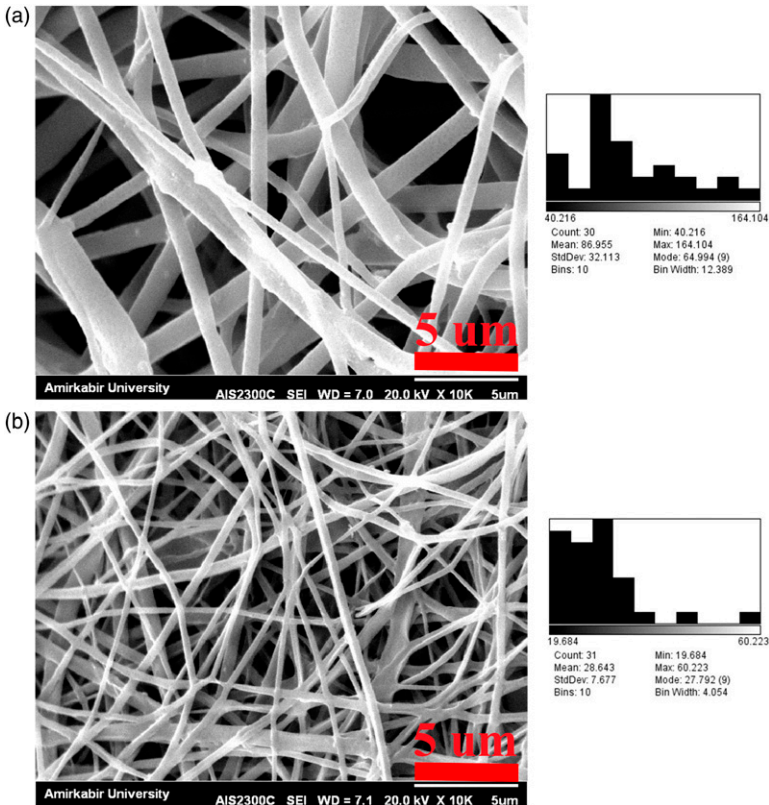


**Figure 2.** SEM image of electrospun nanofibers (a) pure PLA, (b) PLA/HA nanofibrous scaffolds.

According to the SEM images of drug-loaded nanofibrous scaffolds shown in [Figure 3](#), the presence of the drug in the scaffolds increased the diameter of the nanofibers, despite the fact that drug concentration has no significant effect on the diameter of the nanofibrous ([Table 2](#)).

### Water absorption

Among the different characteristics of tissue engineering scaffolds, water absorption is a substantial property to be studied. [Figure 4](#) shows the water absorption results after 24 and 48 h, and shows that the PLA/HA composite nanofibrous scaffolds have higher water absorption than pure PLA nanofibrous scaffolds. In addition, drug-loaded nanofibrous scaffolds significantly have higher water absorption capacity.

Water absorption results showed that PLA/HA composite nanofibrous scaffolds have higher water absorption than pure PLA nanofibrous scaffolds. This is due to the increase in the hydroxyl groups of the composite structure. Over time, water permeability in the polymer chains increases, which leads to enhancement in swelling and water absorption. In addition, the high hydrophilicity of scaffolds ameliorates interaction between cells and

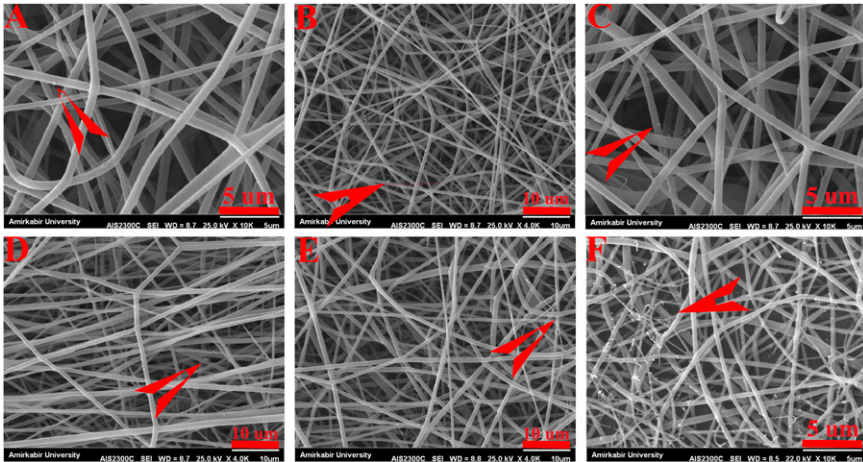


**Figure 3.** SEM images of drug-loaded nanofibrous. Red arrows demonstrate the drug molecule in scaffolds. A, B, C, D, E, and F refer to samples P0.05, P0.1, P0.2, P0.5, P1, and P2, respectively.

**Table 2.** Sample codes and the mean diameters of fibers.

Samples	PLA	PLA/HA	P0.05	P0.1	P0.2	P0.5	P1	P2
Average diameter (nm)	92.94	35.14	61.95	56.98	63.24	62.03	62.31	31.38
±SD.	38.54	12.63	14.58	19.21	20.15	23.12	23.12	11.89

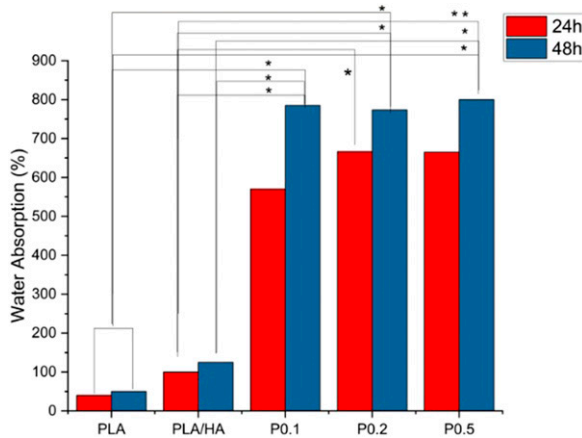


**Figure 4.** Water absorption behavior of samples at 24 h and 48h ( $p < 0.05$ ).

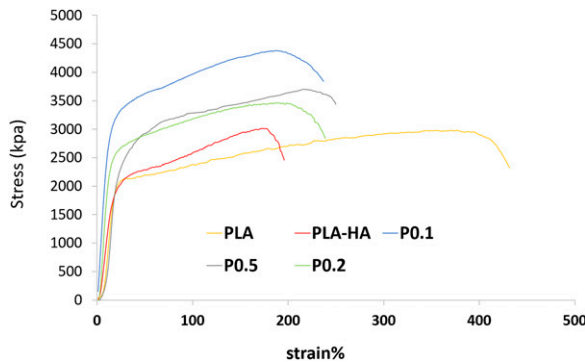


**Figure 5.** Stress-strain curves of PLA, PLA/HA, and PLA/HA containing MP nanofibrous scaffolds.

scaffolds.<sup>12</sup> Other studies that have examined electrospun scaffolds containing HA have also confirmed that the hydrophilicity significantly increases in fibers.<sup>57,59</sup> The primary findings of our investigation are comparable to those of Nia et al.<sup>34</sup>

According to FTIR and SEM results of MP-loaded fibers (Figure 3), the drug had been loaded successfully. Water absorption analysis clearly shows the interaction between the increasing contents of the drug and the water absorption capacity of the fibers. This finding could be due to the presence of the hydrophilic drug in the fiber's structure, which causes the scaffolds to absorb more water.<sup>47</sup> Furthermore, such a design would alter the degradation process of scaffolds. Since more water absorption capacity means that the water could penetrate the scaffold more rapidly. Consequently, the thin firm aligns nanofibers start to degrade, and the structure becomes curly amorphous.

### Mechanical properties

A study of the tensile behavior of the PLA/HA composite scaffolds shows that failure strain is significantly reduced compared to the pure PLA scaffolds. A stress-strain curve of the PLA-HA electrospun scaffold is shown in Figure 5, showing an ultimate tensile strength (UTS) of 2.9 MPa for the PLA/HA fibrous mat at a maximum elongation of 180%. Maximum elongation was recorded for pure PLA (~400%) scaffold (ultimate tensile strength of 2.75 MPa), but the maximum UTS belongs to the PLA/HA composite (2.9 MPa), and in the composite containing MP maximum UTS was 4.35 MPa (Table 3).

The results showed that the maximum UTS is related to P0.1 composite scaffolds. This increase is probably due to the fiber diameter decrease (from 90 nm to 60 nm) because the fiber tensile strength at the nanoscale is very different and increases with decreasing fiber diameter.<sup>60,61</sup> Also, Chanda et al.<sup>57</sup> showed that the presence of HA on electrospun polycaprolactone and chitosan scaffolds did not significantly change the tensile strength, but the reduction of elongation at the breaking point was noticeable. Kerns et al. reported that the fresh human tibial nerve elongation is 40% and peroneal nerve is 60%. Also, the ultimate tensile strength for tibial nerve is  $3.91 \pm 0.92$  and peroneal nerve is  $3.88 \pm 1.41$  MPa.<sup>62</sup> The results of this study demonstrated an ultimate tensile strength of 4.35–3.4 MPa for the P0.1-P0.5 and

**Table 3.** Sample codes, ultimate tensile strength, and the maximum elongation.

Samples	PLA	PLA/HA	P0.1	P0.2	P0.5
Ultimate tensile strength (UTS) (MPa)	2.75	2.9	4.35	3.42	3.7
Maximum elongation (%)	400	180	194	209	218

elongation of 194–218%, which are close to the tibial nerve and peroneal nerve. So, this composite may be a promising candidate for nerve scaffolds in terms of mechanical properties.

### Degradation test

SEM micrographs prepared during degradation analysis showed no specific variation in pure PLA scaffolds after 28 days, but in the nanofibers of PLA/HA composite scaffolds, a morphological variation was seen. Nanofiber deformation, swelling, and expansion were observed in composite scaffolds as the incubation time increased, and the fibrous surface structure faded (Figure 6).

Burdick et al. reported that complete HA degradation occurs in less than 40 days,<sup>63</sup> whereas less than 4% of the PLA scaffold is degraded within 40 days.<sup>64</sup> Complete degradation of the scaffold occurs in more than 12 months.<sup>65</sup> In our composite scaffolds, the presence of HA, due to its high degradation rate, accelerates the process of scaffold degradation over 28 days. Other research has found that the presence of HA in a structure accelerates the rate of deterioration.<sup>12,57,66</sup>

The swelling ratio definitely influences the degradation behavior of scaffolds. On the one hand, SEM images of the drug-loaded nanofibrous scaffolds clearly show that after 2 weeks, the scaffold is partially degraded. On the other hand, the mass loss percentage of the MP-loaded fibers is significantly higher than PLA or PLA/HA fibers. Conclusively the higher drug percentage in the nanofibrous leads to faster degradation.

The influence of drug concentration on the rate of degradation was investigated within a week. The result clearly shows that the more drugs loaded, the faster scaffolds degrade (Figure 7 And Figure 8.). As previously described, more drug content leads to more water absorption due to more hydrophilic groups in structure.<sup>47</sup> Since one of the major mechanisms for degradation is diffusion and water could penetrate the composite structure rapidly, so the degradation will occur sooner. Figure 9 depicts the degradation of sample P0.5 over 2 weeks.

### Drug release studies

The released amounts of MP from the PAL/HA electrospun fibers were obtained spectrophotometrically at 260 nm by a UV spectrophotometer during 14 days' incubation in PBS. The correlation between MP and absorbance was determined using the following equation:

$$y = 4.5392x - 0.4474(R^2 = 0.997) \quad (4)$$

Where, x is the MP concentration ( $\mu\text{g/mL}$ ), and y is the optical density (OD) value measured, respectively.

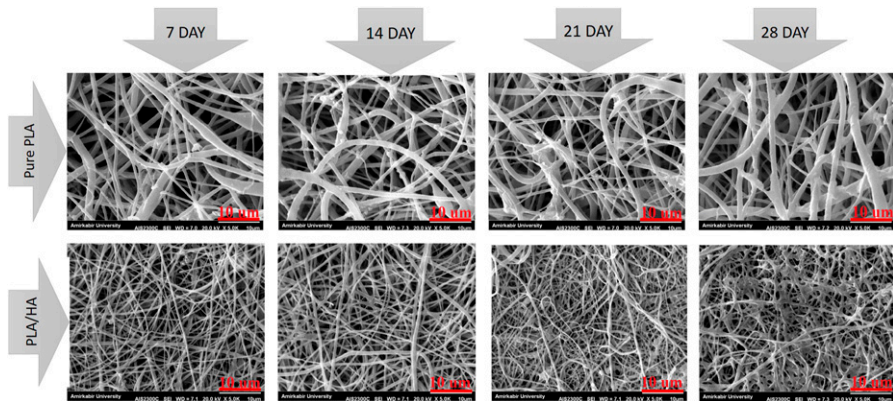


**Figure 6.** SEM image of scaffolds biodegradability up to 28 days.

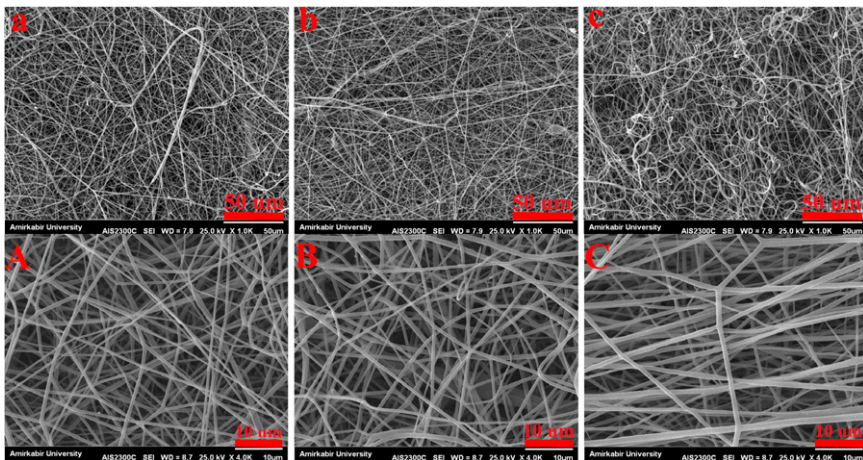


**Figure 7.** Effect of drug concentration on degradation A, B, C) refer to P0.1, P0.2, and P0.5, respectively on day 0. a, b, c) refer to the same samples, respectively in 1 week.

As shown in [Figure 10](#), the release pattern from the PLA/HA nanofibers showed an initial burst release in the first few hours, followed by slower release rates. Notably, after 350 h the percentage of MP release from PLA/HA nanofibrous scaffolds with different MP percentages from 0.05 to 2%, were 96, 91, 74, 31, 21, and 15%, respectively. In addition, the maximum percentage of MP release from the PL/HA nanofibers was recorded at 0.05% MP. Conversely, the MP release percentage was lowest when the MP concentration was 2%.

An initial burst release in the MP release profile may be attributed to the high degradation rate of hyaluronic acid in the composite nanofibers, similar to studies by



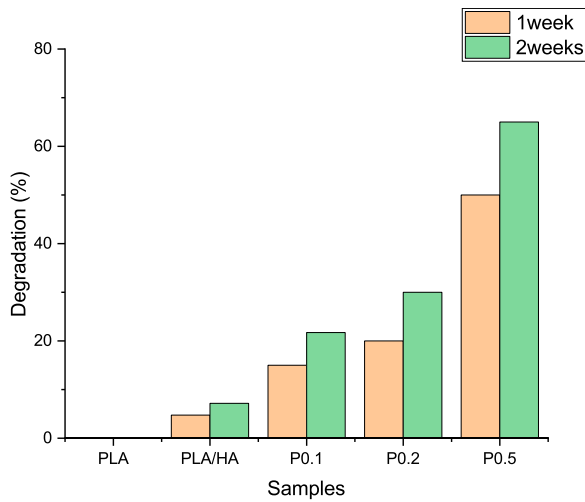


**Figure 8.** Degradation behavior of different samples during 2 weeks.

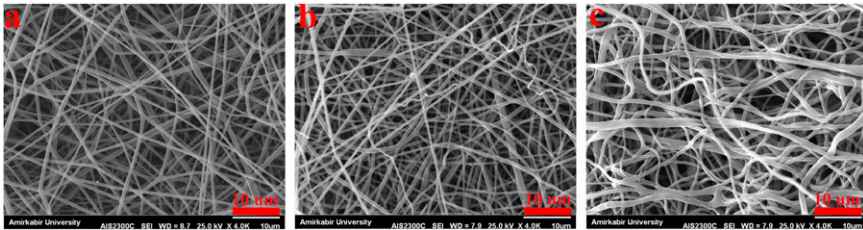


**Figure 9.** Effect of time on degradation of drug-loaded fiber (a) P0.1 on day 0 (b) P0.1 on day 7 (c) P0.1 on day 14.

Entekhabi et al.,<sup>12,63</sup> and consequently, a higher specific surface area of the nanofibrous scaffolds containing HA.<sup>67</sup> When the MP concentration was 2%, the MP release percentage was at a minimum. This may be due to the fact that when the MP percentage was at its maximum, the dissolution rate in the electrospinning solution decreased.

There is a decreasing trend in drug release with an increasing concentration of MP. An experimental study done by pitarresi,<sup>68</sup> shows that increasing MP:PLA/HA ratio resulted in less drug release in PBS solution, similar to our findings. In a related study by Jafari-aghdam et al.<sup>69</sup> MP was loaded in an electrospun nanofibrous. Their drug release profile in which the accumulated drug release will decrease with increasing drug concentration, is as same as our study. It could be due to the physicochemical properties of MP, because its structure is crystalline,<sup>70</sup> and as Fu JC<sup>71</sup> demonstrated, an increase in the degree of crystallinity of the polymeric fibrous scaffolds would decrease the polymer diffusivity.

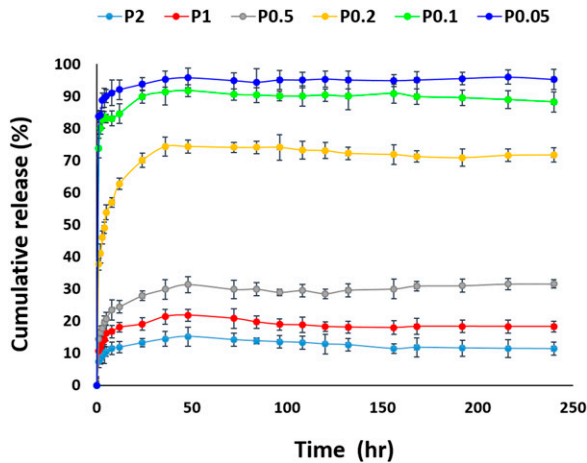


**Figure 10.** Cumulative release of MP from the PLA/HA nanofibrous scaffolds.

Since the primary mechanism of drug release is diffusion and PLA is semi-crystalline,<sup>72</sup> increasing the MP concentration could make the fibrous structure more crystalline, and the drug release rate decreases. In addition, as literature shows, the drug molecule can interact with polymers.<sup>73</sup> This observation of the drug release profile is almost certainly due to the binding affinity between the hydroxyl group of MP and the functional groups of hyaluronic acid.

On the one hand, SEM images of higher MP concentration indicate the changes in nanofibrous structure. More drug contents lead to more roughness in the nanofibrous (Figure 3), which is probably the morphological effect of bonding between MP and hyaluronic acid. On the other hand, the drug release trend declares that loading more contents of MP will result in fewer released drug molecules because more drug molecules engage with the polymers and the chance of bonding is undoubtedly higher. This hypothesis is similar to the previous literature, which asserts that when a steroid-like MP is loaded physically or covalently with hyaluronan, the *in vitro* drug profile will altered.<sup>74</sup>

### Cell culture

The MTT assay was used to study the metabolic activity of the Schwann cells (SCs) on PLA/HA nanofibrous scaffolds containing MP. The results in Figure 11 significantly revealed that the composite scaffolds containing MP increase the growth and viability of SCs compared to the control group. Despite the fact that drug-loaded fibers have poorer cell survival than PLA or PLA/HA fibers, statistical analysis shows no significant difference between the optimum drug concentration (P0.5) and PLA or PLA/HA fibers. Figure 12 shows the morphology of SCs on the scaffolds. As can be seen, the cells' adhesion to the scaffold and the proliferating SCs is quite evident.

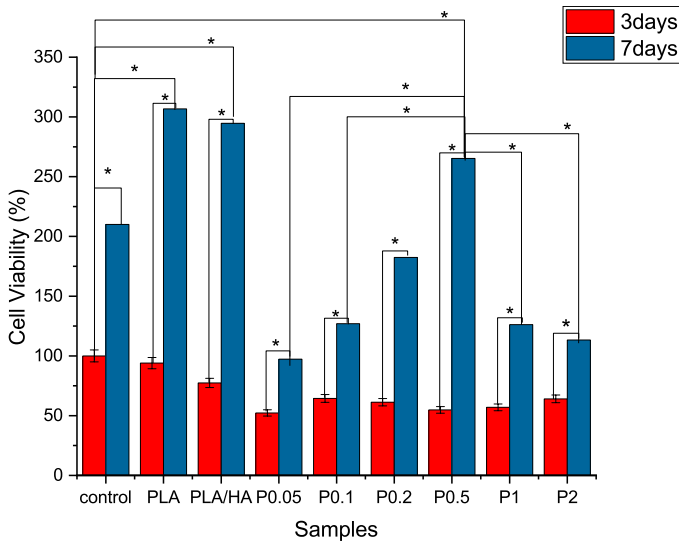


**Figure 11.** MTT analysis of MP-loaded PLA/HA nanofibrous scaffold.

Previous research carried out by Solis et al. showed that HA interacts with cell surface receptors such as RHAMM and CD44.<sup>26</sup> Hence, HA-based scaffolds have been used as nerve guidance conduits and scaffolds for peripheral nerve regeneration, while the combination of HA with other polymers can improve its cell adhesion properties. Chen et al. reported axonal regrowth into SCs grafts enhanced when MP is administered at the time of spinal cord transection and SC implantation.<sup>75</sup> The PLA/HA nanofibrous scaffold with optimum MP concentrations has a positive effect on the growth and viability of SCs, while the scaffolds with a higher percentage of MP showed less cell bioavailability at 3 and 7 days.

The ability of cells to adhere and proliferate on scaffolds is influenced mainly by the morphology of electrospun fibers. The use of electrospun scaffolds and synthetic polymers that can modify fiber morphology is based on the fact that cells can grow on the scaffold in the same way they do on the ECM.

Also, the cell attachment on the scaffold was evaluated via SEM. The image of scaffolds containing Schwann cells shows good interaction between SCs and scaffolds and cell division seen in these images, which indicates the suitable condition of the cell on the scaffolds.

As Belkas et al. stated, in natural nerve tissue, Schwann cells prosper nerve regeneration by secreting neurotrophic factors and ECM components.<sup>76</sup> So providing a scaffold with ECM-based components to mimic the natural environment of Schwann cells will accelerate nerve regeneration. In regards, it can be seen in [Figure 12](#), that the Schwann cell secreted their natural ECM components.

As can be seen from [Figure 12](#) and [Figure 13](#), after 2 days of cell cultivation, the SCs spreading on the scaffolds were greater than the control (glass coverslips) because of the

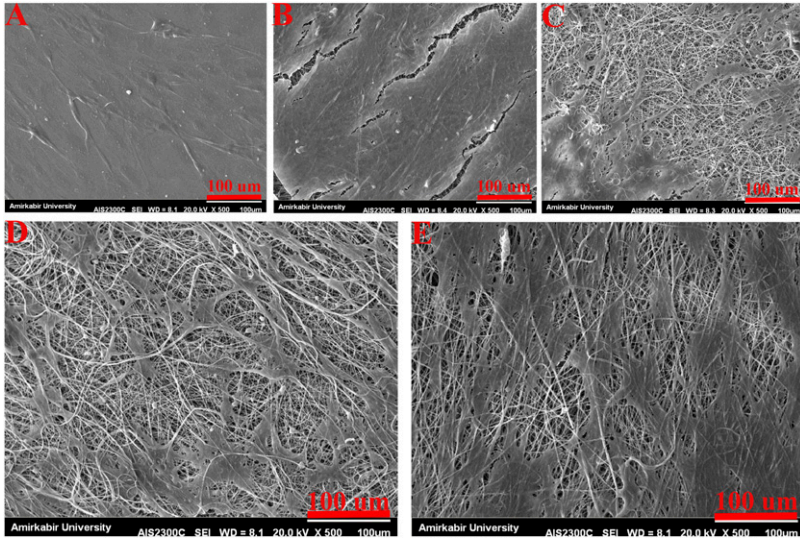


**Figure 12.** Attachment of SCs on nanofibrous scaffolds X500. (a) control (b) PLA (c) PLA/HA (d) P0.2 (e) P0.5.

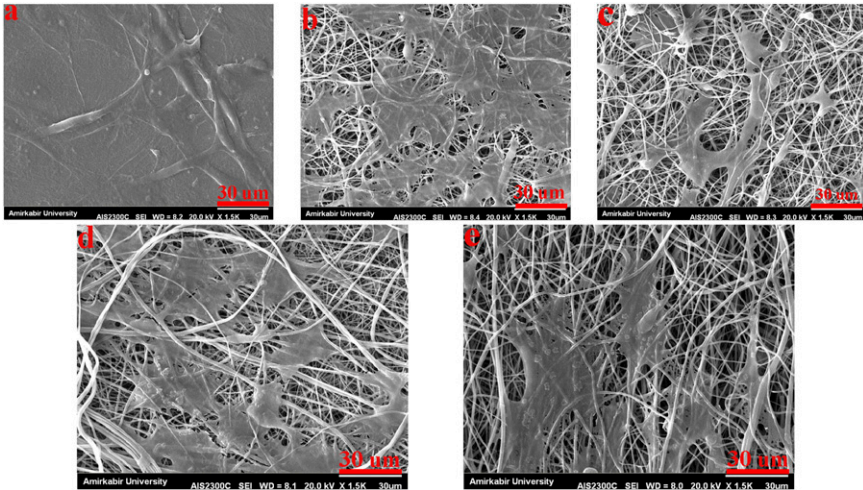


**Figure 13.** Attachment of SCs on nanofibrous scaffolds X = 1500. (a) control (b) PLA (c) PLA/HA (d) P0.2 (e) P0.5.

high specific surface area and appropriate hydrophilicity of the samples, leading to a good adhesion between the cells and scaffolds. On day second, the cell growth on the P0.5 scaffolds was better than other scaffolds which is in accordance with MTT results.

In vitro results indicate that low values of MP (lower than 5000 ppm) can lead to improving SCs viability on the nanofibrous scaffolds, while higher MP may play a negative role in the SCs viability. Therefore, it may be concluded that optimum percentages of MP are effective for nerve tissue repair. In this study, samples containing 0.5 w/v MP are the optimal scaffold.

## Conclusion

Pure PLA and PLA/HA nanofibrous composite scaffolds were fabricated by the electrospinning method, and their physicochemical and biological properties were studied. The results indicated that PLA/HA nanofibrous scaffolds have better biochemical and biomechanical properties than pure PLA. Subsequently, MP-loaded PLA/HA nanofibrous scaffolds were prepared. The results of this study declare that the water absorption capacity of MP-loaded nanofibrous increases approximately 7-fold than PLA/HA composite and biodegradation will occur at a faster rate when drug concentration increases. This finding along with morphological and drug release profiles intensifies the notion of drug-polymers interaction. Cell adhesion and in vitro results showed that novel MP-loaded electrospun nanofibers had appropriate biological features and good biocompatibility. The overall investigation of MP-containing scaffolds showed that incorporating the optimum amount of MP may positively affect Schwann cell behaviors, promising in soft tissue regeneration.

## Acknowledgements

The authors acknowledge funding from Sina Trauma and Surgery Research Center, Tehran University of Medical Sciences.

## Declaration of conflicting interests

The author(s) declared no potential conflicts of interest with respect to the research, authorship, and/or publication of this article.

## Funding

The author(s) received no financial support for the research, authorship, and/or publication of this article.

## ORCID iDs

Masoumeh Haghbin Nazarpak  <https://orcid.org/0000-0002-3248-974X>

Somaye Akbari  <https://orcid.org/0000-0003-2081-7758>

## References

1. Lotfi L, Khakbiz M, Moosazadeh Moghaddam M, et al. A biomaterials approach to Schwann cell development in neural tissue engineering. *J Biomed Mater Res A* 2019; 107: 2425–2446.
2. Hay ED. *Cell biology of extracellular matrix*. Springer Science & Business Media, 2013.
3. Alhosseini SN, Moztaarazadeh F, Mozafari M, et al. Synthesis and characterization of electrospun polyvinyl alcohol nanofibrous scaffolds modified by blending with chitosan for neural tissue engineering. *Int J Nanomedicine* 2012; 7: 25–34.
4. Salehi M, Naseri-Nosar M, Ebrahimi-Barough S, et al. Sciatic nerve regeneration by transplantation of Schwann cells via erythropoietin controlled-releasing polylactic acid/multiwalled carbon nanotubes/gelatin nanofibrils neural guidance conduit. *J Biomed Mater Res B: Appl Biomater* 2018; 106: 1463–1476.
5. Polo Y, Luzuriaga J, Iturri J, et al. Nanostructured scaffolds based on bioresorbable polymers and graphene oxide induce the aligned migration and accelerate the neuronal differentiation of neural stem cells. *Nanomedicine: Nanotechnology, Biol Med* 2021; 31: 102314.
6. Sun X, Bai Y, Zhai H, et al. Devising micro/nano-architectures in multi-channel nerve conduits towards a pro-regenerative matrix for the repair of spinal cord injury. *Acta Biomater* 2019; 86: 194–206.
7. Mobasser A, Faroni A, Minogue BM, et al. Polymer scaffolds with preferential parallel grooves enhance nerve regeneration. *Tissue Eng A* 2015; 21: 1152–1162.
8. Aurand ER, Lampe KJ, Bjugstad KB, et al. Defining and designing polymers and hydrogels for neural tissue engineering. *Neurosci Res* 2012; 72: 199–213.
9. Hoffman-Kim D, Mitchel JA, Bellamkonda R V, et al. Topography, cell response, and nerve regeneration. *Annu Rev Biomed Eng* 2010; 12: 203–231.
10. Santoro M, Shah SR, Walker JL, et al. Poly (lactic acid) nanofibrous scaffolds for tissue engineering. *Adv Drug Deliv Rev* 2016; 107: 206–212.
11. Uppal R, Ramaswamy GN, Arnold C, et al. Hyaluronic acid nanofiber wound dressing—production, characterization, and in vivo behavior. *J Biomed Mater Res Part B: Appl Biomater* 2011; 97: 20–29.
12. Entekhabi E, Nazarpak MH, Moztaarazadeh F, et al. Design and manufacture of neural tissue engineering scaffolds using hyaluronic acid and polycaprolactone nanofibers with controlled porosity. *Mater Sci Eng C* 2016; 69: 380–387.
13. Meghana B, Umesh D, Abhay S, et al. Electrospinning nanotechnology-A robust method for preparation of nanofibers for medicinal and pharmaceutical application. *Asian J Pharm Res Develop* 2020; 8: 176–184.
14. Geller HM and Fawcett JW. Building a bridge: engineering spinal cord repair. *Exp Neurol* 2002; 174: 125–136.
15. Schmidt CE and Leach JB. Neural tissue engineering: strategies for repair and regeneration. *Annu Rev Biomed Eng* 2003; 5: 293–347.
16. Lopes MS, Jardini AL, Maciel Filho R, et al. Poly (lactic acid) production for tissue engineering applications. *Proced Eng* 2012; 42: 1402–1413.
17. Yao Q, Cosme JGL, Xu T, et al. Three dimensional electrospun PCL/PLA blend nanofibrous scaffolds with significantly improved stem cells osteogenic differentiation and cranial bone formation. *Biomaterials* 2017; 115: 115–127.

18. Gómez-Pachón EY, Vera-Graziano R and Campos RM. Structure of poly (lactic-acid) PLA nanofibers scaffolds prepared by electrospinning. *IOP Conf Ser Mater Sci Eng* 2014; 12003.
19. Singh D, Babbar A, Jain V, et al. Synthesis, characterization, and bioactivity investigation of biomimetic biodegradable PLA scaffold fabricated by fused filament fabrication process. *J Braz Soc Mech Sci Eng* 2019; 41: 121.
20. Singhvi MS, Zinjarde SS, Gokhale D V, et al. Polylactic acid: synthesis and biomedical applications. *J Appl Microbiol* 2019; 127: 1612–1626.
21. Liu S, Qin S, He M, et al. Current applications of poly (lactic acid) composites in tissue engineering and drug delivery. *Composites B: Eng* 2020; 199: 108238.
22. Collins MN and Birkinshaw C. Hyaluronic acid based scaffolds for tissue engineering—A review. *Carbohydr Polym* 2013; 92: 1262–1279.
23. Fraser JRE, Laurent TC, Laurent UBG, et al. Hyaluronan: its nature, distribution, functions and turnover. *J Intern Med* 1997; 242: 27–33.
24. Voigt J and Driver VR. Hyaluronic acid derivatives and their healing effect on burns, epithelial surgical wounds, and chronic wounds: a systematic review and meta-analysis of randomized controlled trials. *Wound Repair Regen* 2012; 20: 317–331.
25. Kuo JW. *Practical aspects of hyaluronan based medical products*. CRC Press, 2005.
26. Solis MA, Chen Y-H, Wong TY, et al. Hyaluronan regulates cell behavior: a potential niche matrix for stem cells. *Biochem Res Int* 2012; 346972.
27. Camenisch TD and McDonald JA. Hyaluronan: is bigger better? *Am J Respir Cell Mol Biol* 2000; 23: 431–433.
28. Chen H, Qin J, Hu Y, et al. Efficient degradation of high-molecular-weight hyaluronic acid by a combination of ultrasound, hydrogen peroxide, and copper ion. *Molecules* 2019; 24: 617.
29. Snetkov P, Zakharova K, Morozkina S, et al. Hyaluronic acid: the influence of molecular weight on structural, physical, physico-chemical, and degradable properties of biopolymer. *Polymers (Basel)* 2020; 12: 1800.
30. Nisbet DR, Crompton KE, Horne MK, et al. Neural tissue engineering of the CNS using hydrogels. *J Biomed Mater Res B: Appl Biomater An Official J The Soc Biomater* 2008; 87: 251–263.
31. Tian WM, Hou SP, Ma J, et al. Hyaluronic acid–poly-D-lysine-based three-dimensional hydrogel for traumatic brain injury. *Tissue Eng* 2005; 11: 513–525.
32. Doblado LR, Martínez-Ramos C, García-Verdugo JM, et al. Engineered axon tracts within tubular biohybrid scaffolds. *J Neural Eng* 2021; 18: 0460c5.
33. Mobasser SA, Terenghi G, Downes S, et al. Schwann cell interactions with polymer films are affected by groove geometry and film hydrophilicity. *Biomed Mater* 2014; 9: 55004.
34. Niu Y, Stadler FJ, Fang J, et al. Hyaluronic acid-functionalized poly-lactic acid (PLA) microfibers regulate vascular endothelial cell proliferation and phenotypic shape expression. *Colloids Surf B: Biointerfaces* 2021; 206: 111970.
35. Chvatal SA, Kim Y-T, Bratt-Leal AM, et al. Spatial distribution and acute anti-inflammatory effects of Methylprednisolone after sustained local delivery to the contused spinal cord. *Biomaterials* 2008; 29: 1967–1975.
36. Nash HH, Borke RC, Anders JJ, et al. Ensheathing cells and methylprednisolone promote axonal regeneration and functional recovery in the lesioned adult rat spinal cord. *J Neurosci* 2002; 22: 7111–7120.

37. Ozturk O, Tezcan AH, Adali Y, et al. Effect of ozone and methylprednisolone treatment following crush type sciatic nerve injury. *Acta Cirurgica Brasileira* 2016; 31: 730–735.
38. Papucci L, Schiavone N, Witort E, et al. Coenzyme q10 prevents apoptosis by inhibiting mitochondrial depolarization independently of its free radical scavenging property. *J Biol Chem* 2003; 278: 28220–28228.
39. Mekaj AY, Morina AA, Bytyqi CI, et al. Application of topical pharmacological agents at the site of peripheral nerve injury and methods used for evaluating the success of the regenerative process. *J Orthopaedic Surg Res* 2014; 9: 1–7.
40. Yüce S, Gökçe EC, Iskdemir A, et al. An experimental comparison of the effects of propolis, curcumin, and methylprednisolone on crush injuries of the sciatic nerve. *Ann Plast Surg* 2015; 74: 684–692.
41. Nachemson AK, Lundborg G, Myrhage R, et al. Nerve regeneration and pharmacological suppression of the scar reaction at the suture site: An experimental study on the effect of estrogen-progesterone, methylprednisolone-acetate and cis-hydroxyproline in rat sciatic nerve. *Scand J Plast Reconstr Surg* 1985; 19: 255–260.
42. Gao W, Chen S, Wu M, et al. Methylprednisolone exerts neuroprotective effects by regulating autophagy and apoptosis. *Neural Regen Res* 2016; 11: 823.
43. Gupta D, Venugopal J, Prabhakaran MP, et al. Aligned and random nanofibrous substrate for the in vitro culture of Schwann cells for neural tissue engineering. *Acta Biomater* 2009; 5: 2560–2569.
44. Croisier F, Duwez A-S, Jérôme C, et al. Mechanical testing of electrospun PCL fibers. *Acta Biomater* 2012; 8: 218–224.
45. Baheiraei N, Yeganeh H, Ai J, et al. Synthesis, characterization and antioxidant activity of a novel electroactive and biodegradable polyurethane for cardiac tissue engineering application. *Mater Sci Eng C* 2014; 44: 24–37.
46. Li B, Shan M, Di X, et al. A dual pH-and reduction-responsive anticancer drug delivery system based on PEG–SS–poly (amino acid) block copolymer. *RSC Adv* 2017; 7: 30242–30249.
47. Shokrollahi M, Bahrami SH, Nazarpak MH, et al. Multilayer nanofibrous patch comprising chamomile loaded carboxyethyl chitosan/poly (vinyl alcohol) and polycaprolactone as a potential wound dressing. *Int J Biol Macromolecules* 2020; 147: 547–559.
48. Rajabi M, Firouzi M, Hossainnejad Z, et al. Fabrication and characterization of electrospun laminin-functionalized silk fibroin/poly (ethylene oxide) nanofibrous scaffolds for peripheral nerve regeneration. *J Biomed Mater Res Part B: Appl Biomater* 2018; 106: 1595–1604.
49. Nategh M, Firouzi M, Naji-Tehrani M, et al. Subarachnoid space transplantation of Schwann and/or olfactory ensheathing cells following severe spinal cord injury fails to improve locomotor recovery in rats. *Acta Med Iranica* 2016; 54: 562–569.
50. Wang Y and Xu L. Preparation and characterization of porous core-shell fibers for slow release of tea polyphenols. *Polymers (Basel)* 2018; 10: 144.
51. Pavia DL, Lampman GM, Kriz GS, et al. *Introduction to spectroscopy*. Cengage Learning, 2008.
52. Reddy KJ and Karunakaran KT. Purification and characterization of hyaluronic acid produced by *Streptococcus zooepidemicus* strain 3523-7. *J BioScience Biotechnol*; 2013.
53. Brenner EK, Schiffman JD, Thompson EA, et al. Electrospinning of hyaluronic acid nanofibers from aqueous ammonium solutions. *Carbohydr Polym* 2012; 87: 926–929.



54. Naghizadeh Z, Karkhaneh A, Khojasteh A, et al. Simultaneous release of melatonin and methylprednisolone from an injectable in situ self-crosslinked hydrogel/microparticle system for cartilage tissue engineering. *J Biomed Mater Res Part A* 2018; 106: 1932–1940.
55. Turanlı Y, Tort S, Acartürk F, et al. Development and characterization of methylprednisolone loaded delayed release nanofibers. *J Drug Deliv Sci Tech* 2019; 49: 58–65.
56. Pattamaprom C, Hongrojjanawiwat W, Koombhongse P, et al. The influence of solvent properties and functionality on the electrospinnability of polystyrene nanofibers. *Macromolecular Mater Eng* 2006; 291: 840–847.
57. Chanda A, Adhikari J, Ghosh A, et al. Electrospun chitosan/polycaprolactone-hyaluronic acid bilayered scaffold for potential wound healing applications. *Int J Biol Macromol* 2018; 116: 774–785.
58. Xie X, Chen Y, Wang X, et al. Electrospinning nanofiber scaffolds for soft and hard tissue regeneration. *J Mater Sci Tech* 2020; 59: 243–261.
59. Snetkov P, Morozkina S, Uspenskaya M, et al. Hyaluronan-based nanofibers: fabrication, characterization and application. *Polymers (Basel)* 2019; 11: 2036.
60. Baji A, Mai YW, Wong SC, et al. Electrospinning of polymer nanofibers: Effects on oriented morphology, structures and tensile properties. *Composites Sci Tech* 2010; 70: 703–718.
61. Arinstein A and Zussman E. Electrospun polymer nanofibers: mechanical and thermodynamic perspectives. *J Polym Sci B: Polym Phys* 2011; 49: 691–707.
62. Kern J, Piponov H, Helder C, et al. Mechanical properties of the human tibial and peroneal nerves following stretch with histological correlation. *The Anatomical Rec* 2019; 11: 2030–2039.
63. Burdick JA, Chung C, Jia X, et al. Controlled degradation and mechanical behavior of photopolymerized hyaluronic acid networks. *Biomacromolecules* 2005; 6: 386–391.
64. Simmons H and Kontopoulou M. Hydrolytic degradation of branched PLA produced by reactive extrusion. *Polym Degrad Stab* 2018; 158: 228–237.
65. Guo Z, Yang C, Zhou Z, et al. *Characterization of biodegradable poly (lactic acid) porous scaffolds prepared using selective enzymatic degradation for tissue engineering.* rsc.org.
66. Lee EJ, Lee JH, Jin L, et al. Hyaluronic acid/poly (lactic-co-glycolic acid) core/shell fiber meshes loaded with epigallocatechin-3-O-gallate as skin tissue engineering scaffolds. *J Nanosci Nanotechnol* 2014; 14: 8458–8463.
67. Garg T, Malik B, Rath G, et al. Development and characterization of nano-fiber patch for the treatment of glaucoma. *Eur J Pharm Sci* 2014; 53: 10–16.
68. Pitarresi G, Palumbo FS, Fiorica C, et al. Injectable in situ forming microgels of hyaluronic acid-g-poly(lactic acid) for methylprednisolone release. *Eur Polym J* 2013; 49: 718–725.
69. Jafari-Aghdam N, Adibkia K, Payab S, et al. Methylprednisolone acetate–Eudragit® RS100 electrospun: preparation and physicochemical characterization. *Artif Cell Nanomedicine, Biotechnol* 2014; 44: 497–503.
70. *Hawley's Condensed Chemical Dictionary*. 6th ed.. John Wiley & Sons, 2016, pp. 692–749. In:
71. Fu JC, Moyer DL, Hagemeyer C, et al. Effect of comonomer ratio on hydrocortisone diffusion from sustained-release composite capsules. *J Biomed Mater Res* 1978; 12: 249–254.
72. Puchalski M, Kwolek S, Szparaga G, et al. Investigation of the influence of PLA molecular structure on the crystalline forms ( $\alpha'$  and  $\alpha$ ) and mechanical properties of wet spinning fibres. *Polymers (Basel)* 2017; 9: 18.

73. Ainurofiq A. Application of montmorillonite, zeolite and hydrotalcite nanocomposite clays-drug as drug carrier of sustained release tablet dosage form. *Indonesian J Pharm* 2014; 25: 125.
74. Goei L, Topp E, Stella V, et al. Polymeric prodrugs: recent experience with devices formed from steroid esters of hyaluronic acid. In: *Polymers in Medicine, Biomedical and Pharmaceutical Applications*. Lancaster: Technomic Publishing Company, 1992, pp. 93–101.
75. Chen A, Xu XM, Kleitman N, et al. Methylprednisolone administration improves axonal regeneration into Schwann cell grafts in transected adult rat thoracic spinal cord. *Exp Neurol* 1996; 138: 261–276.
76. Belkas JS, Shoichet MS, Midha R, et al. Peripheral nerve regeneration through guidance tubes. *Neurol Res* 2004; 26: 151–160.